WENOCLAW: A Higher Order Wave Propagation Method

David I. Ketcheson[1] and Randall J. LeVeque[2]

[1] University of Washington ketch@amath.washington.edu
[2] University of Washington rjl@amath.washington.edu

1 Introduction

Many important physical phenomena are governed by hyperbolic systems of conservation laws

$$\mathbf{q}_t + f(\mathbf{q})_x = 0, \tag{1}$$

for which a wide range of numerical methods have been developed. In this paper we present a numerical method for solution of (1) that is also applicable to general hyperbolic systems of the form

$$\mathbf{q}_t + A(\mathbf{q}, x, t)\mathbf{q}_x = 0. \tag{2}$$

In the nonlinear, nonconservative case, the method may be applied if the structure of the Riemann solution is understood. Examples of (1-2) include acoustics and elasticity in heterogeneous media. Wave-propagation methods of up to second order accuracy have been developed and applied to such systems ([4, 5]).

Many high order accurate methods for solution of (1) have been developed, including the essentially non-oscillatory (ENO) and weighted ENO (WENO) schemes. Such methods rely on calculating fluxes, and may not be applied to the more general system (2).

The method described in this work combines the notions of wave propagation and the method of lines, and can in principle be extended to arbitrarily high order accuracy by the use of high order accurate spatial reconstruction and a high order accurate ODE solver. In this work, we use Runge-Kutta methods.

The method is implemented in a software package, WENOCLAW, that is based on CLAWPACK [6] and makes use of Riemann solvers in the same form required for CLAWPACK. The software package and additional documentation are freely available at

http://www.amath.washington.edu/~claw/

2 One-dimensional Discretization

2.1 Semi-discretization

Many numerical methods have been developed to approximately solve (1) based on Godunov's method. The method relies on solving Riemann problems, which consist of (2) with piecewise constant initial data

$$q(x,0) = q_0(x) = \begin{cases} q^- & \text{if } x < 0 \\ q^+ & \text{if } x > 0. \end{cases} \tag{3}$$

The conservation law is integrated over a cell to obtain

$$\frac{\partial Q_i}{\partial t} = -\frac{1}{\Delta x}(f(q^*_{i+\frac{1}{2}}) - f(q^*_{i-\frac{1}{2}})), \tag{4}$$

where $q^*_{i-\frac{1}{2}}$ is the solution to the Riemann problem along the ray $x = x_{i-\frac{1}{2}}$ (or equivalently, $f(q^*_{i-\frac{1}{2}})$ is the Godunov flux) and Q_i is the average of q over the ith grid cell. High order accuracy can be achieved using equation (4) as follows. First, reconstruct a piecewise polynomial approximation $\tilde{q}_i$ to q_i in each cell. In particular, obtain reconstructed values

$$q^+_{i-\frac{1}{2}} = \tilde{q}_i(x_{i-\frac{1}{2}}) = q^e(x_{i-\frac{1}{2}}) + \mathcal{O}(\Delta x^p) \tag{5}$$

$$q^-_{i+\frac{1}{2}} = \tilde{q}_i(x_{i+\frac{1}{2}}) = q^e(x_{i+\frac{1}{2}}) + \mathcal{O}(\Delta x^p) \tag{6}$$

which are approximations to q at the neighboring cell interfaces. Here q^e denotes the exact solution.

If the Godunov flux at $x_{i+\frac{1}{2}}$ is then obtained by solving a Riemann problem with left and right states $q^-_{i-\frac{1}{2}}$ and $q^+_{i-\frac{1}{2}}$, respectively, the resulting semi-discrete approximation (4) is accurate to order p.

Similar to the approach in ([4]), we now proceed to rewrite (4) in terms of fluctuations. Given a system of the form (2), we assume that the solution to the Riemann problem is a similarity solution consisting of a set of waves moving at constant speeds. For nonlinear systems where this may not be the case, we assume the use of an approximate Riemann solver that yields such a solution. This class of solvers includes linearized (such as Roe) solvers, as well as the simpler HLL and LLF solvers. In any case, we then have a decomposition of the jump in the Riemann problem into waves:

$$\Delta q = q_r - q_l = \sum_{p=1}^{M_w} \mathcal{W}^p, \tag{7}$$

where $\mathcal{W}^p$ is the jump across the pth wave, M_w is the number of waves, and each wave has an associated wave speed s^p.

We wish to express the flux difference in (4) in terms of fluctuations, $\mathcal{A}^\pm \Delta q$. The fluctuations may be defined in terms of the flux function:

$$\mathcal{A}^- \Delta q = f(q^*) - f(q^-) \tag{8}$$
$$\mathcal{A}^+ \Delta q = f(q^+) - f(q^*), \tag{9}$$

where $\Delta q_{i-\frac{1}{2}} = q^+_{i-\frac{1}{2}} - q^-_{i-\frac{1}{2}}$. Notice that the fluctuations are a splitting of the flux difference:

$$f(q^+_{i-\frac{1}{2}}) - f(q^-_{i-\frac{1}{2}}) = \mathcal{A}^+ \Delta q_{i-\frac{1}{2}} + \mathcal{A}^- \Delta q_{i-\frac{1}{2}}. \tag{10}$$

The sum on the right hand side of (10) is denoted by $\mathcal{A}\Delta q_{i-\frac{1}{2}}$ and referred to as a total fluctuation.

More generally, the fluctuations may be defined in terms of the waves:

$$\mathcal{A}^+ \Delta q_{i-\frac{1}{2}} = \sum_{p=1}^{m} (s^p_{i-\frac{1}{2}})^+ \mathcal{W}^p_{i-\frac{1}{2}} \tag{11}$$
$$\mathcal{A}^- \Delta q_{i+\frac{1}{2}} = \sum_{p=1}^{m} (s^p_{i+\frac{1}{2}})^- \mathcal{W}^p_{i+\frac{1}{2}} \tag{12}$$

The fluctuation $\mathcal{A}^- \Delta q$ represents the net effect of all left-going waves on the solution, while $\mathcal{A}^+ \Delta q$ represents the net effect of all right-going waves.

Using Eqns. (8-9), the flux difference in Eqn. (4) can be rewritten as

$$f(q^*_{i+\frac{1}{2}}) - f(q^*_{i-\frac{1}{2}}) = \mathcal{A}^- \Delta q_{i+\frac{1}{2}} + f(q^-_{i+\frac{1}{2}}) + \mathcal{A}^+ \Delta q_{i-\frac{1}{2}} - f(q^+_{i-\frac{1}{2}}) \tag{13}$$

We now interpret $q^+_{i-\frac{1}{2}}$ and $q^-_{i+\frac{1}{2}}$ as the left and right states, respectively, for a Riemann problem within cell i. Then we have

$$f(q^-_{i+\frac{1}{2}}) - f(q^+_{i-\frac{1}{2}}) = \mathcal{A} \Delta q_i \tag{14}$$

where $\Delta q_i = q^-_{i+\frac{1}{2}} - q^+_{i-\frac{1}{2}}$. Substitution of (14) into (13) gives

$$f(q^*_{i+\frac{1}{2}}) - f(q^*_{i-\frac{1}{2}}) = \mathcal{A}^- \Delta q_{i+\frac{1}{2}} + \mathcal{A}^+ \Delta q_{i-\frac{1}{2}} + \mathcal{A} \Delta q_i. \tag{15}$$

Substitution into (4) yields the semi-discrete scheme

$$\frac{\partial Q_i}{\partial t} = -\frac{1}{\Delta x}(\mathcal{A}^- \Delta q_{i+\frac{1}{2}} + \mathcal{A}^+ \Delta q_{i-\frac{1}{2}} + \mathcal{A} \Delta q_i). \tag{16}$$

Notice that the final term on the right hand side of (16) does not require the solution of a Riemann problem. It is clear from the derivation that this scheme reduces to the corresponding flux-differencing scheme when applied to (1). The advantage of the scheme over flux-differencing schemes lies in the ability to solve systems of the form (2). Since systems of this form generally cannot be rewritten in terms of a flux function, fluctuations are calculated in terms of the decomposition (11-12). Alternatively, the f-wave decomposition of [2] may be used to obtain the fluctuations.

Derivation of the scheme directly from (2), without the use of a flux function, is omitted here for the sake of brevity. The scheme (16) remains valid as long as the Jacobian A is constant (as a function of x) within each cell.

2.2 Reconstruction

In the previous section, we assumed that high order accurate point values of the solution were known. In fact, at the beginning of a time step, only cell-averaged quantities are known. We now discuss the problem of reconstructing point values.

Many details are omitted here; the reader is referred to [1] for details on WENO reconstruction and to [5] for details on TVD reconstruction.

Suppose we have a formula for obtaining the high order accurate approximations (5-6) for a scalar function $q(x)$. We will further assume that the formula can be written as

$$q^+_{i-\frac{1}{2}} = Q_i + \phi^+(\theta_{i+s_1-\frac{1}{2}}, ..., \theta_{i+s_2-\frac{1}{2}})\Delta q_{i-\frac{1}{2}} \tag{17}$$

$$q^-_{i-\frac{1}{2}} = Q_{i-1} + \phi^-(\theta_{i+s_1-\frac{1}{2}}, ..., \theta_{i+s_2-\frac{1}{2}})\Delta q_{i-\frac{1}{2}} \tag{18}$$

where s_1, s_2 are parameters defining the stencil of the method and

$$\theta_{j-\frac{1}{2}} = \frac{\Delta q_{j-\frac{1}{2}}}{\Delta q_{i-\frac{1}{2}}}. \tag{19}$$

For instance, in the case of minmod reconstruction we have

$$\phi^\pm = \mp\frac{1}{2}\left(1 + \text{sgn}(\theta_{I-\frac{1}{2}})\right)\min(1, |\theta_{I-\frac{1}{2}}|) \tag{20}$$

where $I - \frac{1}{2}$ is the next interface upwind of $i - \frac{1}{2}$.

This scalar reconstruction may be applied to systems of equations in various ways. In the simplest approach, the scalar reconstruction is applied to each component of $\mathbf{q}$. This approach works well for some problems, but in other cases it is insufficient. In particular, it appears to become successively less satisfactory as the order of accuracy of the reconstruction is increased. See [7] for a detailed discussion with respect to central WENO schemes, for instance.

Accuracy can be improved by instead applying the reconstruction to the characteristic fields of $\mathbf{q}$. To do so, we reconstruct as follows. Let $A_{i-\frac{1}{2}} = A(q, x_{i-\frac{1}{2}})$. Let $r^p_{i-\frac{1}{2}}, l^p_{i-\frac{1}{2}}$ be the right and left eigenvectors of $A_{i-\frac{1}{2}}$. First each jump Δq is decomposed into characteristic components θ^p. Then $\mathbf{q}$ is reconstructed via

$$\mathbf{q}^+_{i-\frac{1}{2}} = Q_i + \sum_p \phi^\pm(\theta^p_{i+s_1-\frac{1}{2}}, ..., \theta^p_{i+s_2-\frac{1}{2}})\alpha^p_{i-\frac{1}{2}} r^p_{i-\frac{1}{2}} \tag{21}$$

where $\alpha^p_{i-\frac{1}{2}} = l^p_{i-\frac{1}{2}} \cdot \Delta q_{i-\frac{1}{2}}$.

The only difference between the following methods is the manner in which the θ's are determined. If the system is nonlinear and/or A has explicit spatial dependence, the reconstruction must account for the variation in the characteristic structure over the stencil.

Wave-Slope Reconstruction

In this approach we first determine the waves entering each cell from the solution of the Riemann problems at each interface using the cell average states. This yields a set of waves $\mathcal{W}^p_{i-\frac{1}{2}}$ associated with each interface. In order to reconstruct $q^{\pm}_{i-\frac{1}{2}}$, we first project the pth wave at each interface in the stencil onto the pth wave at $x_{i-\frac{1}{2}}$:

$$\theta^p_{j-\frac{1}{2}} = \frac{\mathcal{W}^p_{j-\frac{1}{2}} \cdot \mathcal{W}^p_{i-\frac{1}{2}}}{\mathcal{W}^p_{i-\frac{1}{2}} \cdot \mathcal{W}^p_{i-\frac{1}{2}}}. \tag{22}$$

We then reinterpret each projected wave as an approximation to the slope of the corresponding characteristic field at that interface.

Typically the waves result from a linearized Riemann solution, so $\mathcal{W}^p_{i-\frac{1}{2}} = (l^p_{i-\frac{1}{2}} \cdot \Delta q_{i-\frac{1}{2}}) r^p_{i-\frac{1}{2}}$. Then we can express $\theta^p_{j-\frac{1}{2}}$ as

$$\theta^p_{j-\frac{1}{2}} = \frac{\alpha^p_{j-\frac{1}{2}}}{\alpha^p_{i-\frac{1}{2}}} \frac{r^p_{j-\frac{1}{2}} \cdot r^p_{i-\frac{1}{2}}}{r^p_{i-\frac{1}{2}} \cdot r^p_{i-\frac{1}{2}}} \tag{23}$$

Characteristic-wise Reconstruction

If the Jacobian A has rapidly varying spatial dependence, the previous methods may yield inaccurate results. In this case, the reconstruction is performed using

$$\theta^p_{j-\frac{1}{2}} = \frac{l^p_{i-\frac{1}{2}} \cdot \Delta q_{j-\frac{1}{2}}}{\alpha^p_{i-\frac{1}{2}}} \tag{24}$$

Transmission-based Reconstruction

In the reconstruction method of the previous section, waves from all characteristic fields at each interface in the stencil are decomposed and contribute to each characteristic field at interface $i - \frac{1}{2}$. For some systems, such as linear acoustics, it appears more reasonable to decompose only waves from the corresponding characteristic field. In the case of acoustics, this has the interpretation of taking waves approaching the interface $i + \frac{1}{2}$ and comparing the part of each that would be transmitted through that interface. In this case, the reconstruction is performed using

$$\theta^p_{j-\frac{1}{2}} = \frac{\alpha^p_{j-\frac{1}{2}}}{\alpha^p_{i-\frac{1}{2}}} (l^p_{i-\frac{1}{2}} \cdot r^p_{j-\frac{1}{2}}). \tag{25}$$

2.3 Time Stepping

Equation (16) may be integrated via an ODE solver. One-step methods are most convenient, and WENOCLAW is implemented using Runge-Kutta methods. Several strong stability preserving methods [3, 9] have been implemented, with order of accuracy ranging from two to five.

3 Extension to Two Dimensions

The semi-discrete scheme may be extended to two dimensions in a straightforward manner. The two-dimensional analog of (2) is

$$\mathbf{q}_t + A(\mathbf{q}, x, y)\mathbf{q}_x + B(\mathbf{q}, x, y)\mathbf{q}_y = 0. \tag{26}$$

It is possible to extend the semi-discrete wave propagation scheme using a simple dimension-by-dimension approach, meaning that the reconstruction at each face only uses data in a slice orthogonal to that face. The scheme is

$$\frac{\partial Q_{i,j}}{\partial t} = -\frac{1}{\Delta x}\left(\mathcal{A}\Delta q_{i,j} + \mathcal{A}^+\Delta q_{i-\frac{1}{2},j} + \mathcal{A}^-\Delta q_{i+\frac{1}{2},j}\right) \tag{27}$$

$$-\frac{1}{\Delta y}\left(\mathcal{B}\Delta q_{i,j} + \mathcal{B}^+\Delta q_{i,j-\frac{1}{2}} + \mathcal{B}^-\Delta q_{i,j+\frac{1}{2}}\right) \tag{28}$$

where the $\mathcal{B}^{\pm}\Delta q$ represent fluctuations in the y direction. Because it neglects certain cross-derivative terms, this scheme is formally of second order, regardless of the order of accuracy of the reconstruction and time stepping. However, in practice, the method yields solutions that are much better than traditional second order methods.

To formally achieve greater than second order accuracy, Gauss quadrature is used to integrate fluctuations over faces. The details of the genuinely multidimensional implementation are omitted here.

4 Sonic Crystal Bandgap Simulation

The semi-discrete wave propagation schemes we have described are especially suited for simulation of high-frequency waves in the presence of rapidly varying material parameters, as is the case for sound waves passing through a sonic crystal.

Small amplitude acoustic waves are described by the linear hyperbolic system

$$p_t + K(x)u_x = 0 \tag{29}$$

$$u_t + \frac{1}{\rho(x)}p_x = 0 \tag{30}$$

where p, u are pressure and velocity perturbations (respectively) relative to some ambient state. Note that this system is of the form (2), with

$$q = \begin{pmatrix} p \\ u \end{pmatrix}, \qquad A = \begin{pmatrix} 0 & K \\ 1/\rho & 0 \end{pmatrix}. \tag{31}$$

We consider a square array of square rods in air with a plane wave disturbance incident parallel to the x-axis. The array is seven periods deep, and periodic boundary conditions are applied in the y-direction. The lattice spacing is 10 cm and the rods have a cross-sectional side length of 4 cm, so that the filling fraction is 0.16. This crystal is similar to one studied in [8], and it is expected that sound waves in the 1200-1800 Hz range will experience severe attenuation in passing through it, while longer wavelengths will not.

The results presented here were calculated using fifth order dimension-by-dimension WENO reconstruction with characteristic-wise limiting and a third order Runge-Kutta method.

Figure 1(a) shows a low frequency plane wave incident from the left. This wave has a frequency of about 800 Hz, well below the partial band gap. As expected, the wave passes through the crystal without significant attenuation. In Figure 2(a), the pressure is plotted along a line approximately midway between rows of rods.

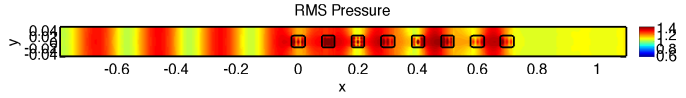

(a) 821 Hz

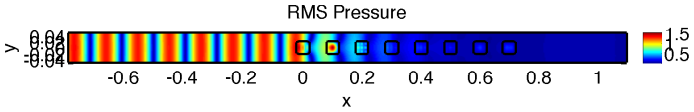

(b) 1600 Hz

Fig. 1. RMS pressure in the sonic crystal.

Figures 1(b) and 2(b) show the same quantities for an incident plane wave with wavenumber $k = 29.22$ m^{-1}, $c = 344$ m/s. Notice that the wave is almost entirely reflected, resulting in a standing wave in front of the crystal.

The authors thank Chi-Wang Shu and Yulong Xing for providing useful sample FORTRAN WENO codes. The first author was supported during this work by a U.S. Department of Homeland Security Fellowship and by a U.S. Department of Energy Computational Science Graduate Fellowship. This research was also supported in part by NSF grant DMS-0106511.

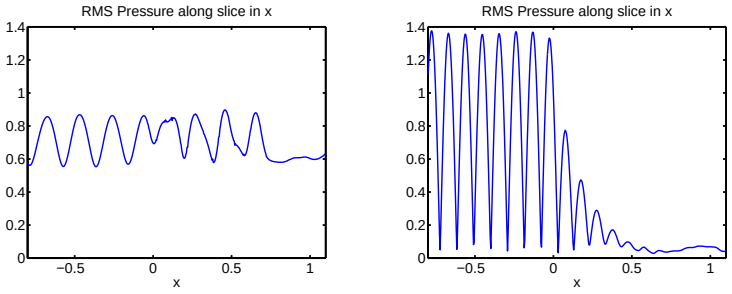

(a) 821 Hz (b) 1600 Hz

Fig. 2. RMS pressure in the sonic crystal along a slice at y=-0.05.

References

1. C.-W. S. B. Cockburn, C. Johnson and E. Tadmor, *ENO and WENO schemes for hyperbolic conservation laws*, in Lecture Notes in Mathematics, A. Quarteroni, ed., vol. 1697, Springer-Verlag, Berlin, pp. 325–432.
2. D. S. Bale, R. J. LeVeque, S. Mitran, and J. A. Rossmanith, *A wave propagation method for conservation laws and balance laws with spatially varying flux functions*, SIAM Journal of Scientific Computing, 24 (2002), pp. 955–978.
3. S. Gottlieb and C.-W. Shu, *Total variation diminishing runge-kutta schemes*, Mathematics of Computation, 67 (1998), pp. 73–85.
4. R. J. LeVeque, *Wave propagation algorithms for multidimensional hyperbolic systems*, Journal of Computational Physics, 131 (1997), pp. 327–353.
5. ———, *Finite Volume Methods for Hyperbolic Problems*, Cambridge University Press, 2002.
6. R. J. LeVeque, *CLAWPACK Version 4.2 User's Guide*, 2003. Available from www.amath.washington.edu/~claw/.
7. J. Qiu and C.-W. Shu, *On the construction, comparison, and local characteristic decomposition for high-order central WENO schemes*, Journal of Computational Physics, 183 (2002), pp. 187–209.
8. L. Sanchis, F. Cervera, J. Sanchez-Dehesa, J. V. Sanchez-Perez, C. Rubio, and R. Martinez-Sala, *Reflectance properties of two-dimensional sonic band-gap crystals*, J. Acoust. Soc. Am., 109 (2001), pp. 2598–2605.
9. R. J. Spiteri and S. J. Ruuth, *A new class of optimal high-order strong-stability-preserving time discretization methods*, SIAM Journal of Numerical Analysis, 40 (2002), pp. 469–491.